

1 **Title: Development of new metrics to assess and quantify climatic drivers of extreme**
2 **event driven Arctic browning.**

3

4 **List of authors:**

Rachael Treharne¹, Jarle W. Bjerke², Hans Tømmervik², Gareth K. Phoenix¹.

¹Department of Animal and Plant Sciences, The University of Sheffield, Western Bank,
Sheffield, S10 2TN, UK

²Norwegian Institute for Nature Research, FRAM – High North Research Centre for Climate
and the Environment, NO-9296 Tromsø, Norway

5 **Corresponding author:**

6 Rachael Treharne¹

¹Department of Animal and Plant Sciences, The University of Sheffield, Western Bank,
Sheffield, S10 2TN, UK

7 rtreharne1@sheffield.ac.uk

8 +44(0)7788765609

9

10 **Keywords:** Arctic, climate change, extreme events, climate metrics, browning, winter,
11 NDVI, heathland, sub-Arctic, ericoid shrubs

12 **Type of Paper:** Primary research article

13 **Abstract (302 words)**

14 Rapid climate change in Arctic regions is resulting in more frequent extreme climatic events.
15 These can cause large-scale vegetation damage, and are therefore among key drivers of
16 declines in biomass and productivity (or “browning”) observed across Arctic regions in recent
17 years.

18 Extreme events which cause browning are driven by multiple interacting climatic variables,
19 and are defined by their ecological impact – most commonly plant mortality. Quantifying the
20 climatic causes of these multivariate, ecologically defined events is challenging, and so existing
21 work has typically determined the climatic causes of browning events on a case-by-case basis
22 in a descriptive, unsystematic manner. While this has allowed development of important
23 qualitative understanding of the mechanisms underlying extreme event driven browning, it
24 cannot definitively link browning to specific climatic variables, or predict how changes in these
25 variables will influence browning severity. It is therefore not yet possible to determine how
26 extreme events will influence ecosystem responses to climate change across Arctic regions.

27 To address this, novel, process-based climate metrics that can be used to quantify the conditions
28 and interactions that drive the ecological responses defining common extreme events were
29 developed using publically available snow depth and air temperature data (two of the main
30 climate variables implicated in browning). These process-based metrics explained up to 63%
31 of variation in plot-level Normalised Difference Vegetation Index (NDVI) at sites in areas
32 affected by extreme events across boreal and sub-Arctic Norway. This demonstrates potential
33 to use simple metrics to assess the contribution of extreme events to changes in Arctic biomass
34 and productivity at regional scales. In addition, scaling up these metrics across the Norwegian
35 Arctic region resulted in significant correlations with remotely-sensed NDVI, and provided
36 much-needed insights into how climatic variables interact to determine the severity of
37 browning across Arctic regions.

38

39 **5.2 Introduction**

40 An increase in frequency of climatic extreme events is among the most marked consequences
41 of climate change (IPCC, 2017). In the Arctic, climate change is progressing faster than almost
42 anywhere else in the world, especially during winter (AMAP, 2017), and increases in extreme
43 events - particularly those associated with winter climate - are therefore being observed
44 (Vikhamar-Schuler et al., 2016, Graham et al., 2017). Although traditionally, climate change
45 research has focussed on changes in mean conditions, it is now recognised that extreme events
46 can have major impacts on ecosystems (Zscheischler et al., 2014, Solow, 2017). In Arctic
47 regions, these impacts include considerable changes in vegetation biomass, productivity and
48 phenology (Bokhorst et al., 2008, Jepsen et al., 2013, Reichstein et al., 2013). However, proper
49 quantitative understanding of the climatic drivers that cause these extreme event impacts is
50 currently lacking, since research has so far focussed on an ‘impact orientated’ approach, where
51 ecological consequences are studied in detail, while climatic drivers are generally defined in
52 qualitative, descriptive terms.

53

54 This is of concern since extreme events linked to winter climate change are already causing
55 major disturbance in the form of sudden mortality and extreme stress in widespread Arctic and
56 sub-Arctic vegetation, with the potential to cause large scale and magnitude impacts, such as
57 the record low productivity of the Nordic Arctic Region (NAR) observed in 2012 (Bokhorst et
58 al., 2009, Bjerke et al., 2014, 2017). Such events include, for example, transient periods of
59 extreme winter warmth, leading to premature dehardening and frost damage (extreme winter
60 warming), or exposure to cold, wind and irradiance following loss of snow cover, leading to
61 severe desiccation damage (frost drought). These are important drivers of ‘Arctic browning’, a
62 decline in biomass and productivity observed across Arctic regions in recent years (Epstein *et*

63 *al.*, 2015, 2016, Phoenix & Bjerke, 2016). However, although remotely sensed Normalised
64 Difference Vegetation Index (NDVI) has been used to assess the extent and impacts of extreme
65 events identified during field studies (Bokhorst et al., 2009), detecting events using this
66 approach is challenging (Treharne et al., 2018). Methods to quantitatively define climatic
67 drivers of extreme event driven browning are therefore needed before the contribution of
68 extreme events to remotely-sensed vegetation change across Arctic regions can be fully
69 determined.

70

71 Extreme events are typically defined using climatological thresholds or using an impact-
72 orientated definition (van de Pol et al., 2017). The latter approach may define an extreme event
73 as one where the ability of an organism to acclimate is substantially exceeded (Gutschick &
74 BassiriRad, 2003) or as a climatologically rare event that alters ecosystem structure or function
75 outside the bounds of normal variability (Smith et al., 2011). Impact orientated definitions are
76 commonly used for ‘compound events’; events driven by combinations of interacting variables
77 which separately may not trigger an extreme response, but, together, cross ecological
78 thresholds to trigger an extreme response (van de Pol et al., 2017). Extreme climatic events
79 which drive Arctic browning, such as frost drought and extreme winter warming, are examples
80 of compound events. These events have therefore so far been defined by their biological
81 impacts; most clearly vegetation mortality (Bokhorst et al., 2011) or a marked visible stress
82 response indicated by persistent anthocyanin pigmentation (Bjerke et al., 2017).

83

84 Events such as these which are defined by an ecological impact and driven by a combination
85 of multiple climatic variables are especially complex to quantify, compare or predict
86 (Easterling et al., 2000). This complexity is compounded when the physiological thresholds
87 beyond which an extreme response is triggered are likely to differ with event timing, preceding

88 conditions and the occurrence of successive events (Knapp et al., 2015, Sippel et al, 2016, Wolf
89 et al, 2016, Ummenhofer & Meehl 2017). This is particularly relevant in Arctic regions, where
90 the depth and extent of insulating snow cover determines whether vegetation is exposed to
91 ambient conditions such as air temperature (Williams et al., 2014; Bokhorst et al., 2016), where
92 event timing may drastically change the conditions to which vegetation is exposed, such as
93 light intensity, and where susceptibility to an extreme response may be heavily dependent on
94 preconditioning, such as the duration of chilling prior to an extreme winter warming event,
95 which could determine susceptibility to premature loss of winter freeze tolerance
96 (dehardening).

97

98 In common with much extreme event literature (Bailey & van de Pol, 2015, Altwegg et al.,
99 2017), assessment of the multivariate climatic drivers in studies of extreme event driven Arctic
100 browning is therefore typically descriptive and unsystematic, dealing with a single event or a
101 few, often differing, events. Nonetheless, these studies have provided critical insights into these
102 events, including a qualitative understanding of event drivers and quantification of major
103 impacts on vegetation growth, phenology and productivity, and on ecosystem CO₂ fluxes
104 (Bokhorst et al., 2008, 2009, 2011; Bjerke et al., 2014, 2017; Parmentier et al., 2018). However,
105 their ability to attribute these measured responses definitively to specific hypothesised climatic
106 drivers is limited. In addition, this approach cannot determine where response thresholds lie,
107 or therefore predict how the severity of the browning response could scale with different
108 climate variables, or when specific conditions might be expected to result in vegetation
109 damage.

110

111 This is of concern given the scale of observed browning impacts, which include substantial
112 loss of biomass at landscape or greater scales (Bjerke et al., 2014, 2017) and large changes in

113 ecosystem CO₂ fluxes with significant implications for landscape-level carbon balance.
114 Furthermore, as the frequency of many types of extreme climatic event is predicted to increase
115 in Arctic regions as climate change progresses, the scale and extent of these impacts are likely
116 to increase (Vikhamar-Schuler et al., 2016, Graham et al., 2017). To fully understand how these
117 events will influence the responses of Arctic ecosystems to climate change, a more systematic
118 approach is needed; correlating measured response to specific, process-based climatic
119 variables. As a first step, a framework to quantify the drivers of extreme event-driven arctic
120 browning, and the interactions between them, is required to understand how variation in these
121 drivers influences the severity of response in vegetation communities, and ultimately drives
122 browning. This quantitative understanding is critical to identify the contribution of extreme
123 events to Arctic browning trends at regional scales, and to fully understand how winter climate
124 change will impact Arctic plant communities.

125

126 Therefore, the aims of this work were to apply established ecological understanding about the
127 drivers of specific instances of extreme event driven browning to (a) identify simple, process-
128 based, quantitative climate metrics that can be used to quantify extreme winter conditions in a
129 systematic, comparable way and (b) assess the relationship between these metrics and changes
130 in satellite NDVI at regional scales. The development of climate metrics initially utilised a
131 dataset of plot-level measurements of NDVI and visible vegetation damage across 19 sites
132 known to have been affected by extreme winter climatic events (primarily frost drought and
133 extreme winter warming experienced during the 2013/14 winter) and subsequent browning.
134 Following this, national meteorological and modelled snow cover datasets were used to
135 compare climate metrics with remotely sensed NDVI across the Norwegian Arctic region. It
136 was hypothesised that (a) simple climate metrics will be identified that correlate with NDVI in
137 areas known to have been affected by browning, (b) these metrics will reflect ecological

- 138 understanding about the mechanisms underlying extreme climatic event driven browning, and
- 139 (c) these metrics will correlate with NDVI change at regional scales.

140 **Methods**

141 **Developing climate metrics using plot-scale analysis**

142 *Plot-level NDVI*

143 Widespread browning of evergreen shrubs across boreal and sub-Arctic regions of Norway was
144 observed following the 2013/14 winter, attributed to extreme winter weather conditions
145 (Meisingset et al., 2015; Bjerke et al. 2017). For this plot-scale analysis, observations of
146 browning recorded in the growing seasons following these extreme winter conditions (2014 or
147 2015) were collated from 19 sites (Fig. 1) in boreal and sub-Arctic Norway. The number of
148 plots at each site ranged from 1 to 143 (with a mean of 19), with each plot measuring 1 x 1m.
149 Replicate plots were located at least 2 m apart and were chosen to reflect the full range of
150 observed browning, including green, healthy vegetation apparently unaffected by extreme
151 events (control plots). Browning at the majority of these sites was driven by the extreme
152 conditions during the 2013/14 winter, with remaining sites browned during previous winters
153 (2011/12 at the earliest; Bjerke et al., 2014). Observations consisted of plot-level NDVI
154 measurements and/or visual assessments of plant damage (mortality; observed as browning).
155 NDVI measurements were taken using either digital NDVI cameras (passive NDVI sensors),
156 in which the usual light sensor is replaced with an infrared sensor, enabling the camera to record
157 visible light in the blue channel and near infrared in the red channel (Llewellyn Data
158 Processing, New Jersey), or an active NDVI sensor (Greenseeker; Trimble, California). The
159 Greenseeker NDVI sensor emits red and infrared light and measures the reflectance of each
160 wavelength in terms of the normalized difference vegetation index (NDVI) and is mainly used
161 in precision agriculture (Bourgeon et al., 2017) and in phenological monitoring; including of
162 browning trends and events in the Arctic (Anderson et al. 2016; Bokhorst et al., 2018). The
163 visual assessments of browning were recorded either as percentage cover of browned

164 vegetation (mortality), or the proportion of the dominant species affected by browning (own
165 data and data provided by J. Bjerke). As NDVI and observed browning (plot survey) were
166 significantly correlated ($p < 0.05$), these correlations (calculated separately across plots within
167 each of three counties) were used to predict plot-level NDVI at plots where observed browning
168 alone, and not NDVI, was recorded.

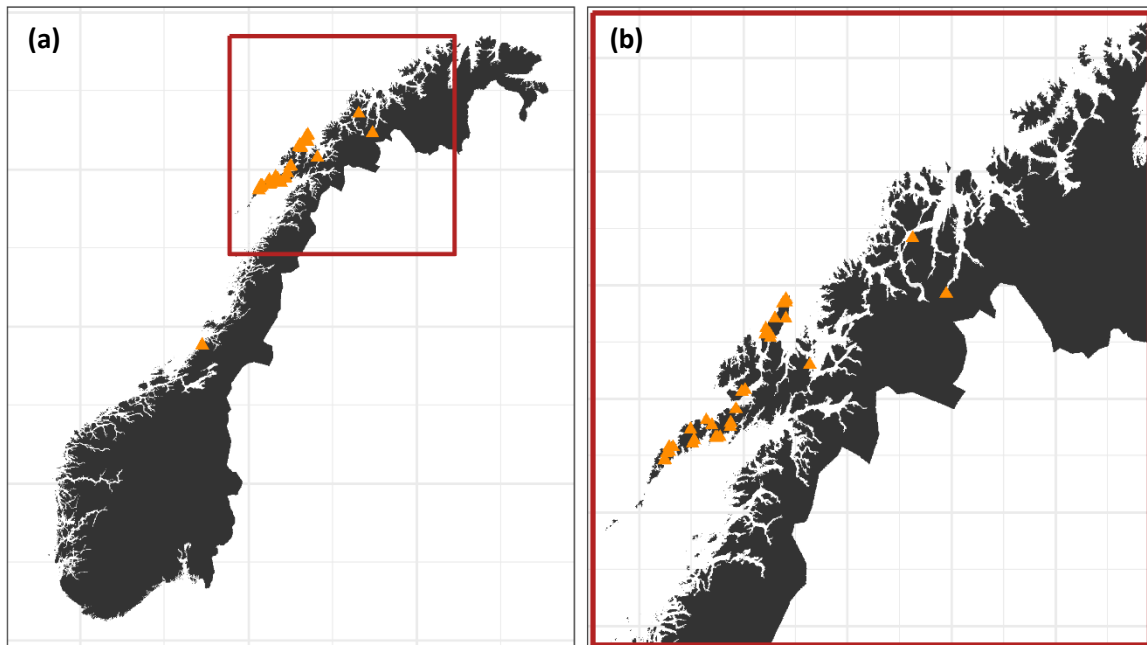


Figure 1: (a) Map of Norway showing locations of 19 sites (orange triangles) where extreme event-driven browning was observed and plot-level NDVI was measured. The Norwegian Arctic Region, the area used for regional level analysis, is outlined in red. This area is shown separately and enlarged in (b).

169

170 To provide data on undamaged controls, a ‘pre-browning’ NDVI value was estimated for each
171 site. To do this, linear regressions of NDVI and observed browning were calculated separately
172 for each county ($p < 0.05$) and used to predict NDVI in vegetation with no observed browning.
173 This approach produced ecologically sensible estimates for healthy dwarf-shrub heathland
174 NDVI of between 0.67 and 0.75 (Street et al., 2007). At two sites, 5-6 NDVI values in adjacent
175 undamaged vegetation (in addition to observed browning plots) were recorded; in these cases
176 recorded NDVI values in undamaged vegetation were averaged to estimate pre-browning

177 values for those sites. Pre-browning NDVI values were assigned to the growing season
178 preceding the winter during which browning occurred (i.e. 2013 for the majority of sites).

179

180 *Climate data*

181 Snow depth maps of Norway with a daily temporal and 1 x 1 km spatial resolution were
182 obtained from The Norwegian Water Resources and Energy Directorate (NVE). This publically
183 available data is produced using the SeNorge snow model (<http://www.senorge.no>), which is
184 forced by daily observations of temperature and precipitation and performs well in Norway
185 (Saloranta, 2012).

186

187 From SeNorge snow maps, daily snow depth values were extracted from each pixel which
188 contained plot-level browning observations in the dataset described above. This data was
189 extracted for each winter between 2011 and 2015. Daily snow depth values were then averaged
190 for each site.

191

192 Daily mean, minimum and maximum air temperature was obtained from the Norwegian
193 Meteorological Institute via the publically available eklima.no web portal. Data for 2011 –
194 2015 was downloaded from the weather stations closest to each site (maximum distance <
195 25km) at an elevation of < 200m (as sites were located in relatively low-lying areas). Based on
196 the quality and availability of air temperature data from these stations, data from 14 stations
197 was subsequently analysed.

198

199 *Development of metrics*

200 Snow and air temperature data was combined into a single dataset. Only data from the winter
201 period was used to develop climate metrics, to avoid any confounding effect of occasional late
202 spring or summer snowfall. To identify an appropriate window for this winter period during
203 which snow cover and cold temperatures could reasonably be expected, and therefore during
204 which warmth and exposure may have ecological consequences, first winter snow fall and final
205 spring snow melt for each winter (2011/12 – 2014/15) were identified. This was done by
206 selecting all periods of absent snow cover (0 mm snow depth) throughout the year; first winter
207 snowfall and final spring melt were recorded as the dates following and preceding the long
208 summer exposure period in consecutive years. Winter was thus defined from Day of Year 305
209 (Day of Winter 1) to Day of Year 120 (Day of Winter 181 or 182).

210

211 Within each winter a set of approaches were used to extract ‘events’ which may have
212 influenced NDVI. These were ‘exposure events’ based on absent snow cover (0 mm snow
213 depth) or ‘warming events’ based on warm winter temperatures ($> 2\text{ }^{\circ}\text{C}$). A $2\text{ }^{\circ}\text{C}$ threshold for
214 warming events was chosen based on visual assessment of temperature data during warming
215 events known to have resulted in browning, and aimed to ensure the full duration of any
216 warming events was considered, while differentiation between short, relatively mild warming
217 events and prolonged periods of high temperatures was facilitated by an ‘intensity’ metric
218 (below and Table 1). Periods of exposure or warming occurring before initial winter snowfall
219 or cold temperatures were excluded. The variables recorded for each event type were chosen
220 based on the mechanism of damage particularly associated with either winter warming (i.e.
221 premature dehardening and initiation of spring-like bud burst, followed by frost damage on the
222 return of cold temperatures) or frost drought (loss of snow cover and subsequent exposure,
223 leading to gradual desiccation as transpiration exceeds uptake from frozen or near-frozen soils)
224 (Table 1). These two processes account for the majority of reported extreme climatic event-

225 driven browning in mainland Norway (e.g. Hørbye, 1882; Printz, 1933; Bokhorst et al., 2009,
226 2012; Bjerke et al. 2014, 2017). Thus, for exposure events (most likely to be associated with
227 frost), event duration, start date and mean air temperature were recorded. For warming events
228 (most likely to be associated with extreme winter warming), a wider range of variables,
229 including the intensity metric, were recorded (Table 1).

230

231 Using this approach, several events were extracted for each year. To select those most likely to
232 influence growing season NDVI, up to 4 events were selected for each year. These were (a)
233 ‘Maximum intensity warming events’; the warming event with the highest ‘Intensity’ (air
234 temperature*duration; Table 5.1), (b) ‘Temperature drop warming events’; the warming event
235 with the greatest 24-h temperature drop following the final day of the event, (c) ‘Maximum
236 duration exposure events’; the maximum duration exposure event (i.e. no snow cover) (d)
237 ‘Maximum warmth exposure events’; the warmest exposure (no snow cover) event.

Table 1: Variables (climate metrics) recorded for each event type (either warming events based on consecutive daily air temperatures of > 2°C, or exposure events based on consecutive days of absent (0mm) snow cover) as extracted from snow depth and air temperature data.

Variable	Meaning	Event type
Count	Event duration (days).	Warming; Exposure
Start date	Date (Day Of Winter) of the first day of the event.	Warming; Exposure
Intensity	Cumulative mean daily air temperature (°C) linearly weighted by duration throughout the event. E.G. for a 3 day event with daily mean air temperatures of 4°C, 6°C and 3°C, Value = (4*1) + (6*2) + (3*3) = 25.	Warming
Mean snow depth	Mean snow depth (mm) during the event.	Warming
Mean air temperature	Mean air temperature (°C) during the event.	Exposure
End minimum temperature	Minimum temperature 24 hours following the final day of the event (°C).	Warming
24 hour temperature drop	Difference between mean daily air temperature on the last day of the event and minimum air temperature 24 hours later (°C).	Warming
5 day temperature mean	Mean daily air temperature over the 5 days following the event (°C).	Warming

238

239

240 *Satellite NDVI*

241 Remotely sensed NDVI data were extracted from the publically available MOD13Q1 version

242 6 dataset. MOD13Q1 provides level 3 16-day composites of vegetation indices at 250 m

243 resolution in a sinusoidal projection. Tiles were downloaded for DOY 193 in 2015, the nearest

244 date to when plot-level measurements were recorded, using USGS Earth Explorer. These tiles

245 were re-projected to the UTM Zone 33 projection using the NASA HDF-EOS To GeoTIFF

246 Conversion Tool (HEG) and mosaicked to encompass the full extent of plot-level data.

247

248 *Statistical analysis*

249 Correlations between metrics representing selected events and subsequent growing season
250 NDVI were assessed by multiple regression. Selection of metrics with high explanatory power
251 for use in multiple regression was initially guided by tree-based regression analysis, following
252 which interactions included in multiple regression of each event type (a – d) against NDVI
253 were based on *a priori* knowledge and predictions relating to the mechanisms through which
254 each event may cause browning (Bokhorst et al., 2008; Bjerke et al., 2017). Terms and
255 interactions without a significant correlation with NDVI change were removed step wise. A
256 maximum of three terms was included in each multiple regression. Plot-level and MODIS
257 NDVI were compared by linear regression.

258

259 **Applying climate metrics at regional scales**

260 The Norwegian Arctic Region (Fig. 1) was selected for upscaling as a clearly definable region
261 encompassing the majority of sites used for plot-level analysis. This area extends southwards
262 to the Arctic Circle (66° 33' N) and eastwards to the longitude of Magerøya, Finnmark (25°
263 40' E); the most northerly point of the Nordic Arctic Region (NAR, Bjerke et al., 2014).

264

265 *5.3.2.1 Satellite NDVI*

266 Both time integrated NDVI (TI-NDVI) and peak/maximum NDVI have been widely used in
267 Arctic vegetation studies (Stow et al., 2004). The TI-NDVI is considered as a robust proxy for
268 total growing-season productivity (Stow et al., 2004; Epstein et al., 2017). Remotely sensed
269 NDVI data were extracted from the publically available MOD13Q1 version 6 dataset described

270 above from the beginning of May (DOY 129) to the end of August (DOY 241). Tiles were
271 extracted for this period in 2014, as the most marked and widespread browning observed at
272 plot-level occurred during the 2013/2014 winter, and from 2005 to 2010 (inclusive) to create a
273 baseline period for comparison. Tiles were re-projected and mosaicked as described above.
274 Unvegetated areas ($NDVI < 0.12$) were masked out. Images were aggregated (by mean) to a 1
275 km resolution to facilitate comparison with climate data.

276 From this May-August NDVI dataset, time-integrated NDVI (TI-NDVI; the sum of NDVI
277 values during this period) was calculated for 2014 and the 2005-2010 baseline period. Change
278 detection was then carried out between 2014 and the 2005-2010 baseline period, producing TI-
279 NDVI change. This process was also carried out for mean July (approximately peak biomass)
280 NDVI.

281

282 *Climate data*

283 Data was obtained from The Norwegian Water Resources and Energy Directorate (NVE) and
284 the Norwegian Meteorological Institute as described above. To provide air temperature data
285 continuously across the Norwegian Arctic region, data was downloaded from every Norwegian
286 Meteorological Institute weather station with an elevation of $< 200\text{m}$ in the counties of
287 Nordland, Troms and Finnmark; a total of 77 stations. The 200m cut-off was used since above
288 this, weather stations tended to be on mountainsides, where data may be less representative of
289 the broader surrounding landscape and so be less suitable for interpolation (the majority of the
290 heathland vegetation typically affected by browning is in low lying regions). Mean daily air
291 temperature from each station was interpolated across these three counties using Inverse
292 Distance Weighted interpolation, before the resulting air temperature map was cropped to the
293 Norwegian Arctic region. Climate data (both air temperature maps and SeNorge snow maps)

294 were resampled using nearest neighbour assignment resampling to correspond to each other
295 and to MODIS data.

296

297 *Climate metrics*

298 Maximum intensity warming events and maximum duration exposure events were chosen to
299 investigate further in this analysis due to their high explanatory power in the plot-level analysis.
300 Extreme event metrics for these two event types were calculated as described above for the
301 2013/2014 winter within each 1 km pixel.

302

303 *Statistical analysis*

304 Multiple regressions of the parameters for each event type were carried out using Generalised
305 Least Squares against TI-NDVI change. This was also done for July NDVI change (change in
306 mid-season NDVI). All regressions were carried out at a 4 km resolution to reduce
307 computational intensity. As the Moran's *I* test indicated significant spatial autocorrelation in
308 model residuals, this was accounted for by using correlated error structures (exponential,
309 Gaussian, linear, spherical and rational quadratic) and selecting the appropriate model error
310 structure (rational quadratic for TI-NDVI and exponential for July NDVI) according to the AIC
311 criterion (Burnham & Anderson, 2002).

312 **Results**

313 **Climate metrics in plot-scale analyses**

314 Climatic events described by simple metrics were well correlated with plot-level NDVI.
315 ‘Maximum intensity warming events’ were calculated as the greatest value within a pixel of
316 sum of daily mean air temperature multiplied by event duration (i.e. intensity) in periods of
317 consistently warm ($> 2^{\circ}\text{C}$) winter air temperatures. The start day in winter, mean snow cover
318 and intensity of these events explained more than 60 % of variation in plot-level NDVI in
319 multiple regression (Fig. 2a; $F = 14.26$, D.F. = 4, 27, $p < 0.001$, $R^2 = 0.63$), with high intensity,
320 later start day and lower mean snow cover corresponding to lower NDVI values. ‘Temperature
321 drop warming events’ were calculated as the periods of consistently warm air temperature ($>$
322 2°C) with the greatest drop in temperature during the 24 hours following the final day of the
323 event. The start day and intensity of these events explained almost 50% of variation in NDVI
324 in multiple regression (Fig. 2b; $F = 10.81$, D.F. = 3, 33, $p < 0.001$, $R^2 = 0.45$). Again, high
325 intensity and later start day were associated with lower NDVI. For both warming event types
326 (maximum intensity warming events and temperature drop warming events) there was a
327 significant interaction between intensity and start day ($p < 0.05$). Tree-based regression
328 analysis (supporting information) of metrics calculated for warming events also highlighted the
329 24-h temperature drop following an event as a metric with high explanatory power for variation
330 in NDVI; mean NDVI in plots which had experienced a maximum intensity warming event
331 with a 24-h temperature drop of more than 5.7°C was 0.2 (NDVI) lower than in those which
332 had not. While the importance of the 24-h temperature drop is of interest and provides some
333 insight into mechanisms underlying plant damage following warming events, its computational
334 complexity (in particular its use of minimum as well as mean air temperature datasets) meant
335 that it was unsuitable for further analysis within this work and was therefore not included in
336 multiple regression analyses.

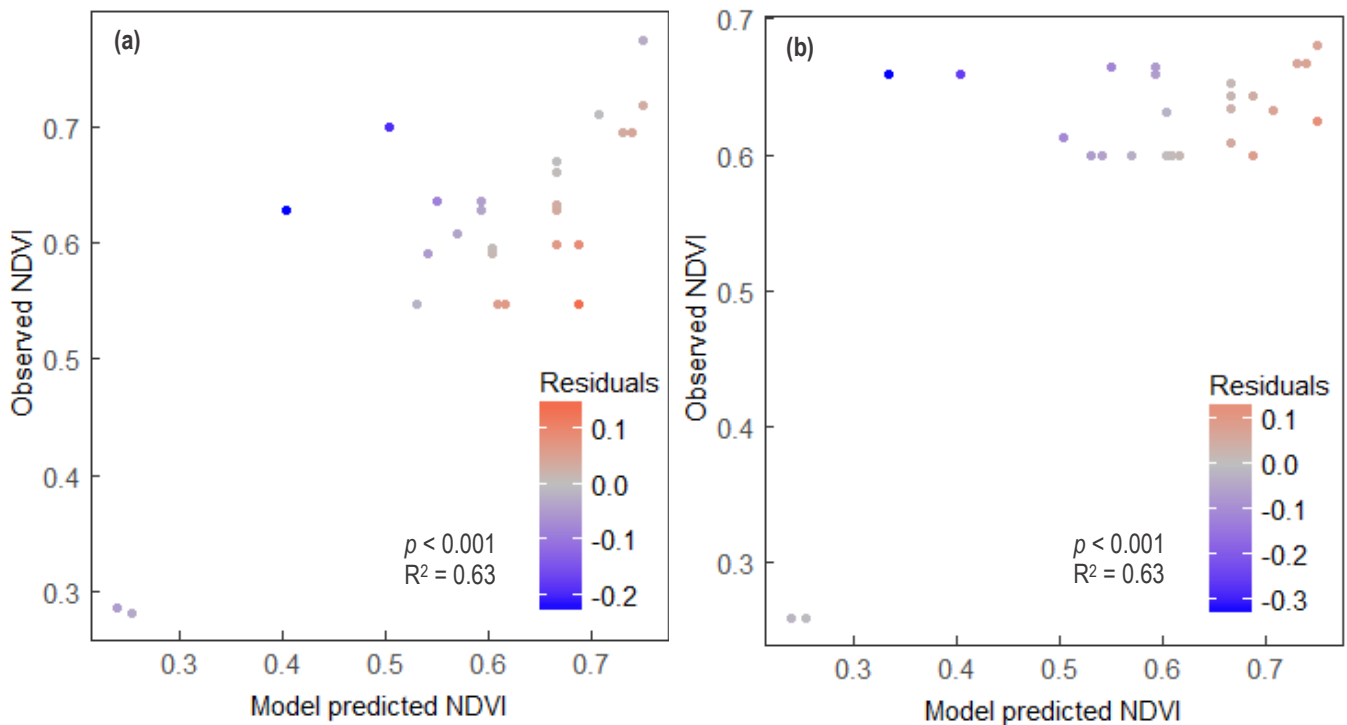


Figure 2: Correlations between plot-level NDVI as predicted by multiple regression models and plot-level NDVI observed in the field. Correlations are shown for (a) ‘Maximum intensity warming events’ and (b) ‘Temperature drop warming events’. Points are coloured according to the value of residuals; warm colouring indicates that multiple regression predicted higher NDVI values than were observed in the field, while cold colouring indicates that multiple regression predicted lower NDVI values than observed.

337

338 ‘Maximum duration exposure events’ were calculated as the periods of consistently absent
 339 snow cover (0 mm snow depth) with the longest duration in days during winter. The start day
 340 of and mean temperature during these events were highly correlated with NDVI in multiple
 341 regression (Fig. 3a; $R^2 = 0.61$, $F = 17.87$, D.F. = 3, 29, $p < 0.001$). ‘Maximum warmth exposure
 342 events’ are the periods of consistently absent snow cover with the highest mean temperature.
 343 The start day and duration of these events were also significantly correlated with NDVI in
 344 multiple regression, albeit with a weaker R^2 (Fig. 3b; $F = 3.802$, D.F. = 3, 29, $p < 0.05$, $R^2 =$
 345 0.21). In both cases there was a significant interaction between the two model predictors (start
 346 day and mean temperature).

347

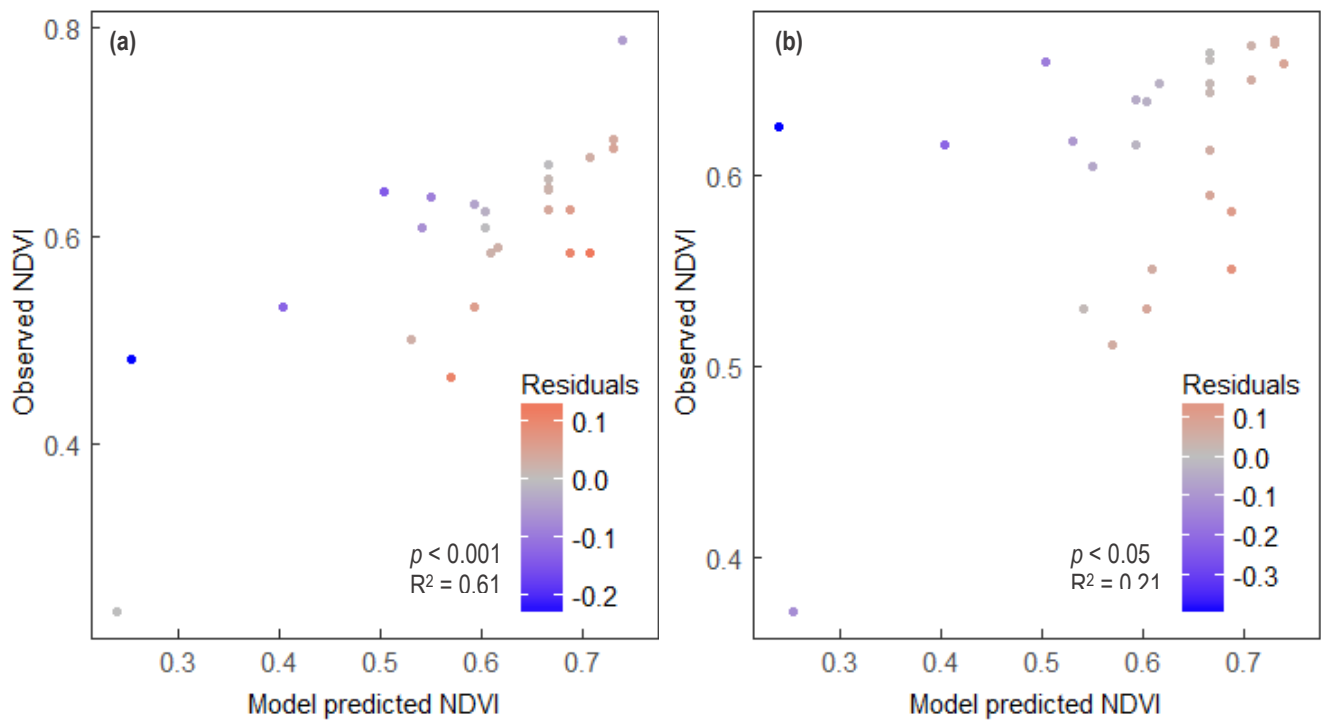


Figure 3: Correlations between plot-level NDVI as predicted by multiple regression models and plot-level NDVI observed in the field. Correlations are shown for (a) ‘Maximum duration exposure events’ and (b) ‘Maximum warmth exposure events’. Points are coloured according to the value of residuals; warm colouring indicates that multiple regression predicted higher NDVI values than were observed in the field, while cold colouring indicates that multiple regression predicted lower NDVI values than observed.

348

349

350 **Climate metrics in regional scale analyses**

351

352 Climate metrics calculated and mapped across the Norwegian ArcticNAR implicate the
 353 processes underlying frost drought and extreme winter warming in MODIS NDVI change
 354 between the 2005-2010 baseline period and 2014. They also highlight interesting
 355 characteristics of winter climate and the conditions which lead to extreme climatic event-driven
 356 browning.

357

358 *Event characteristics*

359 Maximum intensity warming event metrics (intensity, start day and mean snow cover) show
360 that prolonged periods of warmth during winter were rare across the Norwegian Arctic region
361 in the 2013/14 winter (indicated by low maximum intensity across much of the region; Fig 4a).
362 Such rare occurrence is consistent with climatic conditions which can produce an ecologically
363 extreme response (i.e. extreme events). The median value of intensity in the 2013/14 winter
364 was 61 across the entire Norwegian Arctic region, compared to a median of 328 specifically in
365 observed browning sites. The wide variation inherent in this variable (with a range of 3 to 2440)
366 across the Norwegian Arctic region means that when mapped, areas where events of especially
367 high intensity took place – reflecting prolonged, unseasonable warmth – are clearly
368 distinguishable by eye (Fig 4a). Visual assessment suggests that high intensity events, when
369 they do occur, are most often found in coastal areas. Furthermore, while most warming events
370 across the region occurred in the first half of the winter period, with 60% occurring in January
371 alone, events with the highest maximum intensity typically began later in the season (Fig 4;
372 best model: R.S.E = 187.24, D.F = 5265; start day: $t = 9.56$, S.E. = 0.07, D.F. = 5265, $p <$
373 0.001). There was no significant correlation between event intensity and mean snow cover
374 during the event.

375

376

377

378

379

380

381

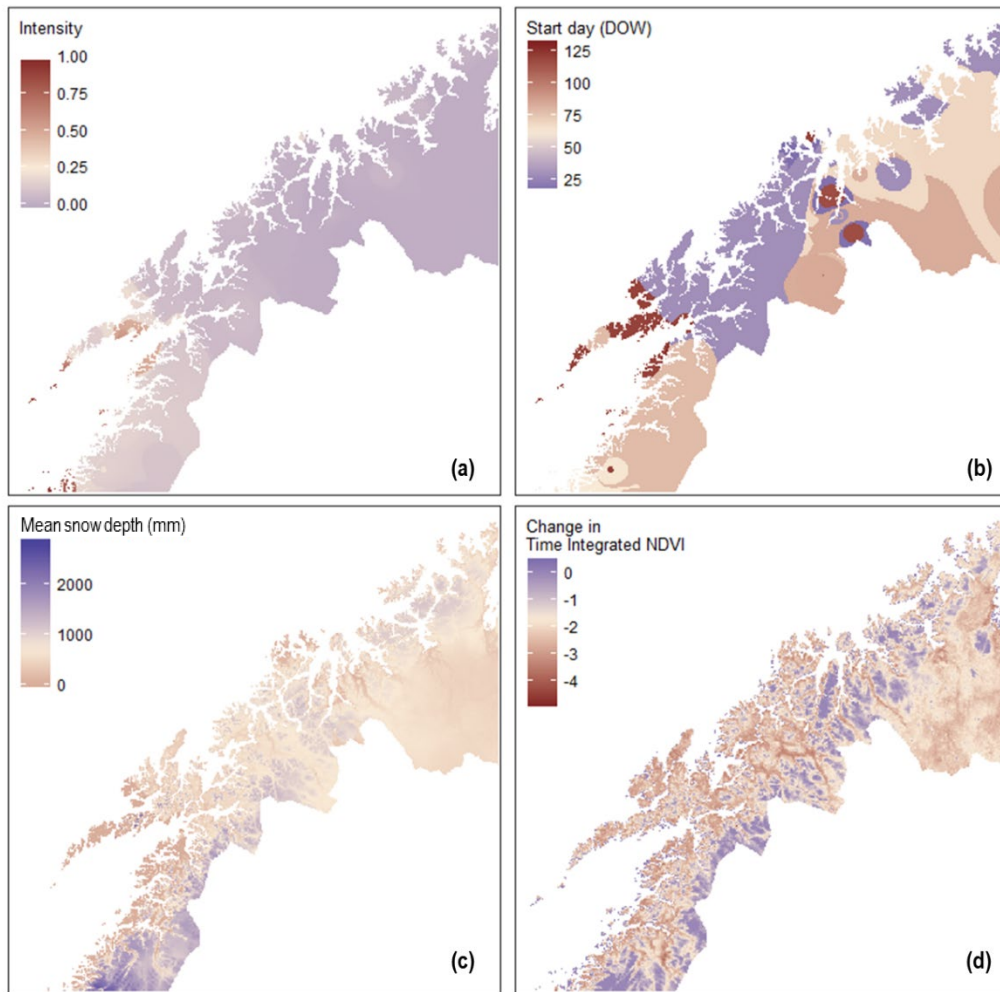


Figure 4: Climate metrics calculated for the warmth event with the highest intensity in each 1 km² pixel. Climate metrics shown are (a) intensity; cumulative warmth weighted linearly by event duration, here rescaled to a range of 0-1 for easier interpretation, (b) the start day of the event (Day of Winter 1 equivalent to Day of Year 305) and (c) mean snow depth (mm) during the event. The change in time integrated NDVI between the baseline 2005-2010 period and 2014 is shown (d) for comparison with the potential climatic drivers (a) – (c).

382

383 Similarly, exposure event metrics show that exposure (snow depth = 0) during winter was
 384 relatively rare across the Norwegian Arctic in the 2013/14 winter (Fig. 5a) and was limited
 385 primarily to coastal areas. Where exposure events did take place further inland, visual
 386 comparison suggests they typically began later in the winter compared to those taking place
 387 close to the coastline (Fig. 5b). All winter 2013/14 exposure events across observed browning
 388 sites plus the majority (59 %) of exposure events across the Norwegian Arctic region were

389 associated with a mean air temperature of more than 0 °C during the event. However, 21 % of
390 Norwegian Arctic-region exposure events were relatively cold, with mean air temperature
391 below or equal to −2 °C. Visual comparison suggests these cold exposure events may be more
392 common further inland. Timing of the longest exposure events across the region was relatively
393 evenly spread throughout the majority of the winter period, although with a higher proportion
394 (32 %) of events occurring in April.

395

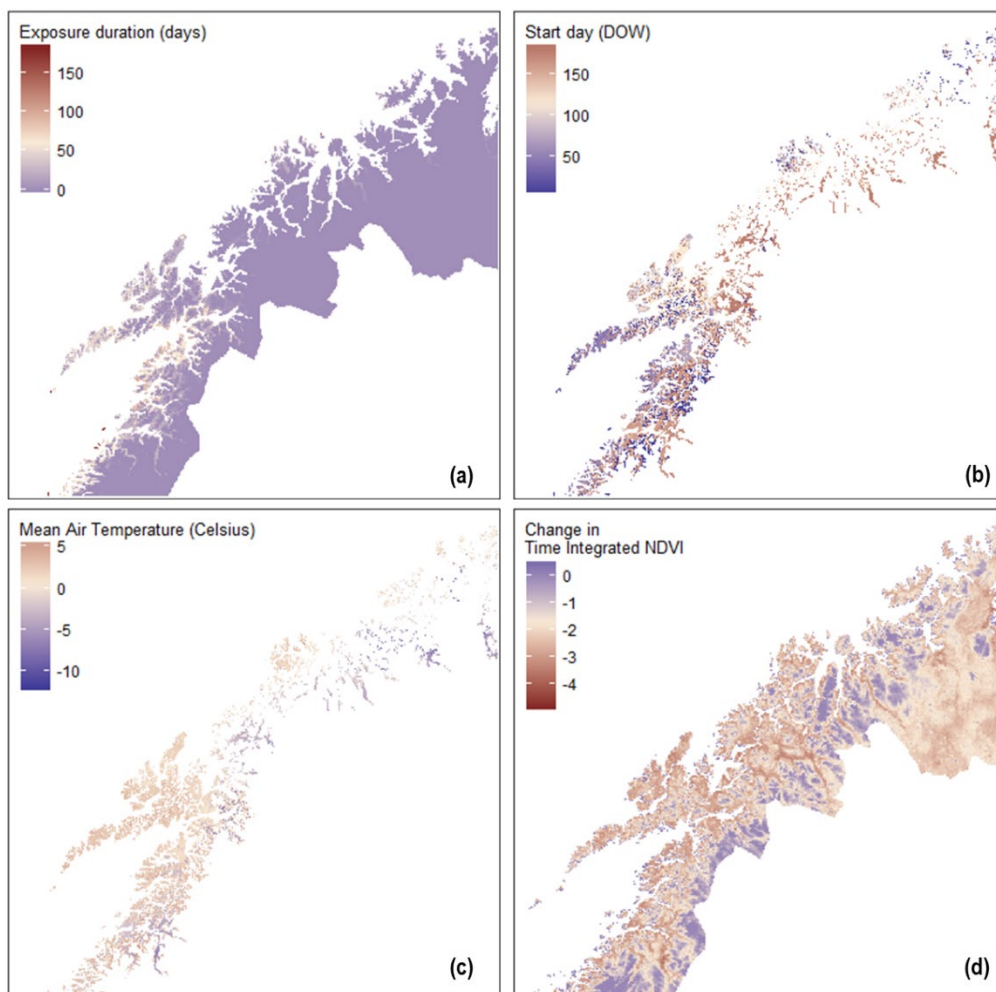


Figure 5: Climate metrics calculated for the exposure event with the longest duration in each 1 km² pixel. Climate metrics shown are (a) event duration (b) the start day of the event (Day of Winter 1 equivalent to Day of Year 305) and (c) mean air temperature (°C) during the event. The change in time integrated NDVI between the baseline 2005-2010 period and 2014 is shown (d) for comparison with the potential climatic drivers (a) – (c).

396

397 *Correlation with MODIS NDVI*

398 *Maximum intensity warm events*: both the intensity of the event (Fig. 4a), and the mean snow
399 cover during the event (Fig. 4c) were significantly positively correlated with change in time
400 integrated NDVI (TI-NDVI), i.e. cooler and shorter warming events with shallower snow
401 resulted in greater negative change in TI-NDVI. (Fig. 4d; best model: R.S.E. = 0.54, D.F. =
402 5259; intensity: $t = 2.1$, S.E. < 0.001, $p < 0.05$; mean snow cover: $t = 13.9$, S.E. < 0.001, $p <$
403 0.001). There was also a significant negative interaction between intensity and mean snow
404 cover ($t = -5.19$, S.E. < 0.001, $p < 0.001$) and, while the start day of the event did not have a
405 significant main effect, there was a significant positive three-way interaction between intensity,
406 mean snow depth and start day (Fig. 6, $t = 2.56$, S.E. < 0.001, $p < 0.05$). Overall, these terms
407 and interactions show that increasing event intensity (greater air temperature * duration) at the
408 shallowest snow depths results in smaller TI-NDVI reductions (Fig. 6, 25 cm line), while at the
409 deepest snow depths increasing event intensity results in greater TI-NDVI reductions (Fig. 6,
410 100 cm line). As winter progresses (moving left to right on Fig. 6), the slope of the relationship
411 between TI-NDVI change and event intensity becomes more positive at any given snow depth;
412 meaning that the threshold of snow depth above which this slope is negative increases.

413

414 There was no correlation between change in peak-season (July) NDVI and any maximum
415 intensity warm event metric.

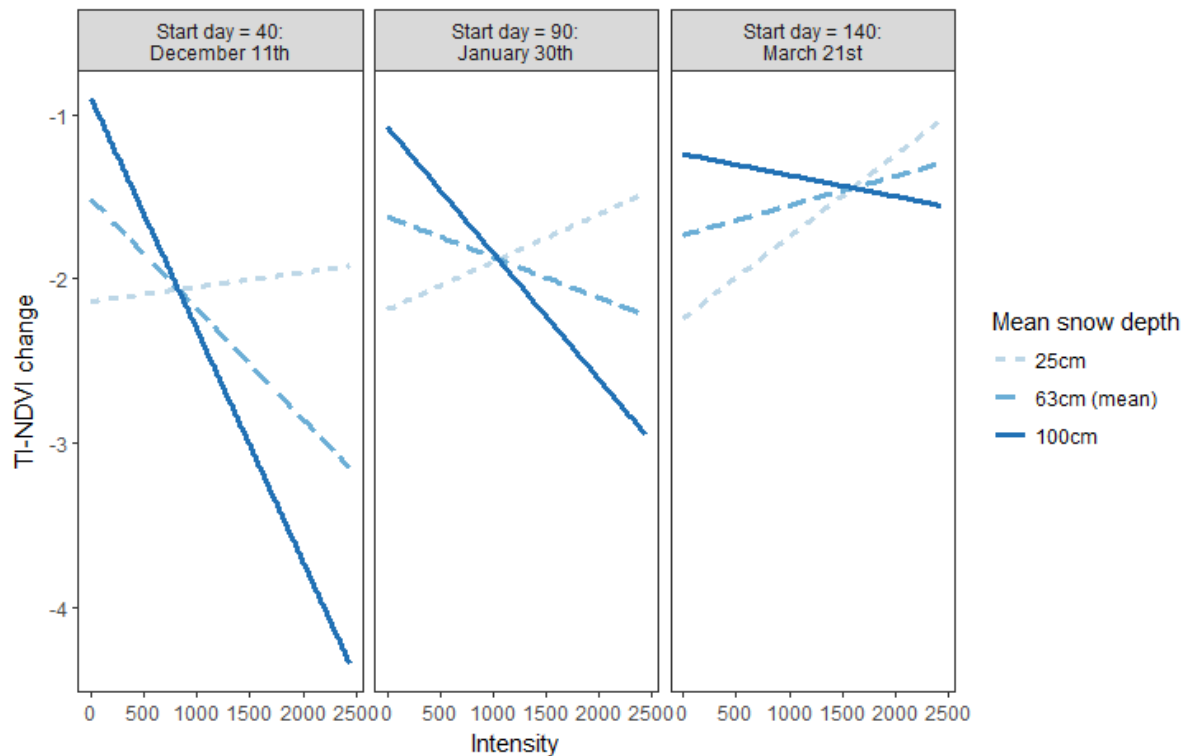


Figure 6: Three-way interaction between intensity (the sum of air temperature multiplied by duration for each day of the event), start day, and mean snow depth in multiple regression of maximum intensity warmth events (the warming event within each pixel with the greatest intensity) with TI-NDVI change. Lines illustrate relationships between event intensity and TI-NDVI change at snow depths of 25cm (short dashed line), the mean value across the Norwegian Arctic Region of 63cm (long dashed line) and 100cm (solid line). Panels show these relationships at different time points during winter.

416

417 *Maximum duration exposure events:* Start day of the longest exposure event (Fig. 5b) was
 418 negatively correlated with change in TI-NDVI, i.e. later longest exposure events resulted in
 419 greater negative NDVI change (best model: R.S.E. = 0.57, D.F. = 2331; start day: $t = -3.91$,
 420 S.E. < 0.001, $p < 0.001$). The mean temperature of the event (Fig. 5c) was positively correlated
 421 with change in TI-NDVI (greater negative TI-NDVI change with cooler events; $t = 3.29$, S.E.
 422 = 0.015, $p < 0.001$), while event duration (Fig. 5a) showed no correlation ($p > 0.05$). There was
 423 an interaction between start day and mean temperature, showing that the slope of the positive

424 relationship between TI-NDVI change and mean temperature became shallower, and
425 eventually became negative, as the winter progressed (Fig. 7 $t = -3.5$, S.E. < 0.001 , $p < 0.001$).

426

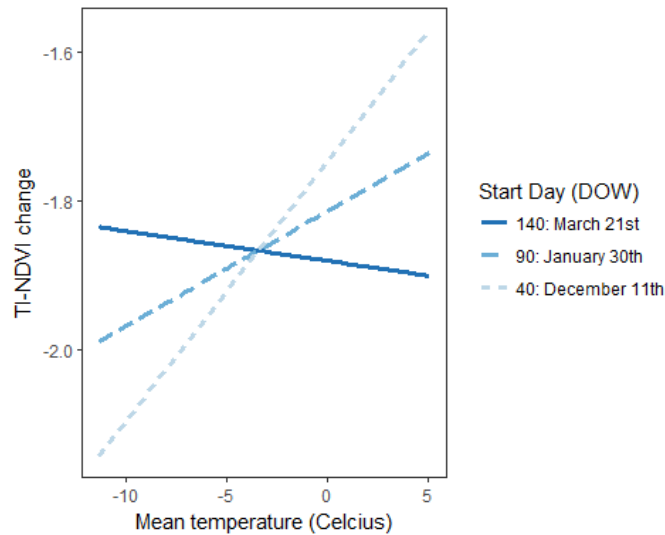


Figure 7: Two-way interaction between the start day and mean air temperature of maximum duration exposure events (periods of consistently absent snow cover with the longest duration in each pixel). Lines illustrate relationships between mean temperature and TI-NDVI change on Day of Winter (DOW) 40 (December 11th; short dashed line), DOW 90 (January 30th; long dashed line) and DOW 140 (March 21st; solid line).

427 There were no correlations between any exposure event metric and change in July NDVI ($p >$
428 0.05).

429

430

431

432

433

434 **Discussion**

435

436 We demonstrate that simple climate metrics can explain variation in NDVI (vegetation
437 greenness) in areas known to have been affected by extreme event-driven arctic browning.
438 These process-based metrics (i) provide quantitative assessment of the climatic conditions that
439 drive browning, and how these combine to do that, showing that periods of unusual warmth
440 and low snow cover during winter are associated with loss of vegetation greenness reinforcing
441 previous descriptive and qualitative assessments of the climatic drivers of browning (Hancock,
442 2008; Bjerke et al., 2014, 2017; Bokhorst et al., 2009; Meisingset et al., 2015), and (ii) provide
443 much-needed insight into how variation in these climate drivers influence the severity of the
444 browning observed. This work also suggests that such metrics, easily calculated from mean
445 daily air temperature and snow depth, could be used to assess the contribution of winter climatic
446 extreme events to Arctic browning at regional scales, and ultimately to improve predictions of
447 how changing Arctic winters will affect the biomass and productivity of vegetation
448 communities.

449

450 **Plot-level analysis**

451 Metrics representing both maximum intensity warming events (the period of consistently
452 warm, $> 2^{\circ}\text{C}$, air temperature with the highest intensity in the plot's pixel, where intensity is
453 the sum of daily mean air temperature multiplied by event duration) and maximum duration
454 exposure events (the period of consistently absent snow cover, 0 mm snow depth, with the
455 longest duration in days in the plot's pixel) explained a high proportion of variation in plot-
456 level NDVI across observed browning sites. In analysis of maximum intensity warm events,
457 high intensity, late start date and shallow snow depth were associated with low NDVI. This is

458 consistent with NDVI and biomass reductions driven by extreme winter warming or frost
459 drought events (Bokhorst et al., 2009, Bjerke et al., 2014; Meisingset et al., 2015). In extreme
460 winter warming, unusual winter warmth causes premature dehardening and initiation of spring-
461 like bud-burst following snow melt and exposure of vegetation to warmth, after which the rapid
462 return of sub-zero temperatures causes frost damage (Phoenix & Lee, 2004; Bokhorst et al.,
463 2008). It is likely that vegetation could be more prone to extreme winter warming damage later
464 in winter, after a substantial cold period has already been experienced and when light levels
465 are increasing, meaning any subsequent warm period is more likely to trigger premature de-
466 hardening and bud-burst (Körner, 2016; Parmentier et al., 2018). Alternatively, frost drought
467 occurs when vegetation is exposed and soils are frozen, which reduces the availability of free
468 water and promotes winter desiccation (Tranquillini 1982; Sakai & Larcher, 2012). In late
469 winter, soils are most likely to be closer to their coldest year-round temperature. Exposure
470 events with a higher mean air temperature at this time may therefore encourage plant
471 transpiration and water loss, but may not be sufficiently warm to initiate soil thaw and an
472 increase in the availability of free water (Larcher & Siegwolf, 1987). Desiccation is likely to
473 be further accelerated in late winter due to higher solar irradiance, which promotes
474 physiological activity including transpiration and increasing water loss (Hadley & Smith, 1986,
475 1989). However, since there is a high explanatory power of the 24-h drop in temperature
476 following the end of the warm period, it appears likely that the browning observed at these sites
477 is driven largely by extreme winter warming rather than frost drought.

478

479 In analysis of maximum duration exposure events, a late start day and comparatively warm
480 mean air temperature (1.7°C) was associated with lower plot-level NDVI, with the negative
481 correlation between mean air temperature and NDVI steepening throughout the winter.
482 Similarly to the above, this could either indicate frost drought or extreme winter warming.

483 Regardless, it would appear that periods of warmth associated with snowmelt or shallow snow
484 depth, particularly in late winter, are strong drivers of the NDVI reductions observed at these
485 sites. This is also consistent with observations that reductions in *Vaccinium myrtillus* biomass
486 in the 2014 growing season in coastal Norway were associated primarily with winter warmth
487 (Meisingset et al., 2015).

488

489 **Regional-scale analysis**

490 Climate metrics calculated for both event types – maximum duration exposure events and
491 maximum intensity warming events – show that both prolonged, warm periods during winter
492 and periods of winter exposure are rare across the Norwegian Arctic region; the majority of the
493 region experienced low maximum intensity of warmth events and no periods of exposure
494 during the 2013/14 winter. This is consistent with ecological theory that states that extreme
495 events should be rare enough that organisms are not (or poorly) adapted to them, such that
496 when these events do occur, an extreme ecological response is produced (Smith 2011). As
497 might be expected, the highest magnitudes of both event types occurred primarily along the
498 coastline, where temperatures are warmer and the climate more variable. As both mean
499 temperatures and temperature variability are expected to increase as climate change progresses
500 (AMAP, 2017), this suggests that coastal areas may act as indicators of conditions likely to
501 become more common as colder, inland areas warm, and supports predictions that the
502 magnitude and frequency of these events will increase across arctic regions as climate change
503 progresses (Vikhamar-Schuler et al., 2016, Graham et al., 2017).

504

505 Climate metrics for both event types correlated with change in TI-NDVI. For maximum
506 duration exposure events the strongest predictor of change in TI-NDVI was mean temperature

507 during the exposure event. However, this relationship changes throughout the winter; the
508 negative correlation between start day and change in NDVI (with later events associated with
509 greater TI-NDVI reductions) is steeper where mean temperature is high. This means that early
510 in the winter, cold exposure events are associated with greater TI-NDVI reductions, but in late
511 winter, from around March, it is warmer events that cause larger TI-NDVI reductions. It is
512 these late winter, relatively warm events which contribute to the largest reductions in TI-NDVI
513 overall. Similarly to the plot-level analysis, this could suggest that in late winter, when
514 vegetation has already experienced cold winter temperatures and light availability is increasing,
515 warm conditions may be more likely to initiate premature dehardening, driving extreme winter
516 warming damage (Bokhorst et al., 2010). However, there is also evidence that the impact of
517 exposure events on change in TI-NDVI may be driven to some extent by frost drought. As
518 described above, mild temperatures and high light levels in late winter could accelerate
519 desiccation by encouraging transpiration and water loss before soils begin to thaw (Parmentier
520 et al., 2018). The contrasting link between TI-NDVI reduction and colder temperatures in early
521 winter suggest greater possibility of frost drought as the driving mechanisms of damage: in
522 early winter when normal air temperatures are higher and soils have had little time to chill, cold
523 exposure events may accelerate or exacerbate soil freezing (Hancock, 2008; Zhao et al., 2017),
524 promoting vegetation desiccation.

525

526 For maximum intensity warmth events the strongest predictor of change in TI-NDVI was mean
527 snow depth during the event. Although, overall, maximum intensity warmth events with
528 shallower snow depths were associated with greater TI-NDVI reductions, the relationship
529 between the severity of these events and change in TI-NDVI was determined by interactions
530 between mean snow depth, start day and the intensity of the event. In early winter, increasing
531 event intensity was associated with greater reductions in TI-NDVI when the mean snow depth

532 during those events was deeper. Also, as winter progresses, the relationship between intensity
533 and TI-NDVI becomes shallower, and by late winter increasing event intensity is associated
534 with greater loss of TI-NDVI only at relatively deep snow depths. Overall, this shows that at
535 low temperatures, shallow snow depth and exposure were consistently associated with greater
536 reductions in TI-NDVI. However, these relationships may also reflect smaller impacts of
537 increasingly severe warm spells in vegetation communities which typically experience shallow
538 snow cover or periods of exposure during winter (for example coastal vegetation communities),
539 compared to those where snow cover is typically deep and persistent (Bokhorst et al., 2016).
540 This would arise where vegetation in areas with normally low snow depth may be more adapted
541 and resilient to fluctuations in winter temperature because they typically are (more likely to be)
542 exposed above the snow (Kudo & Hirao, 2006, Bienau et al., 2014). Increasing warming event
543 intensity in these vegetation communities may therefore have little effect. In contrast, areas
544 with greater snow depth may be much more sensitive to extreme temperature fluctuations and
545 higher rates of water loss associated with exposure since here vegetation is typically covered
546 by deep snow throughout winter, and hence is less well adapted to exposure. Further work
547 should determine whether amount of snowmelt (i.e. initial snow depth – final snow depth)
548 during a warming event may be a more ecologically relevant metric than mean snow depth.

549

550 It is not clear why the relationship between change in TI-NDVI and event intensity is positive
551 in late winter, even at mean snow depth (i.e. less negative TI-NDVI change with greater
552 intensity). This may be related to the alleviation of water stress from snow melt-water, or to
553 the impact of increased soil moisture following snowmelt on phenology (Vaganov et al., 1999;
554 Barichivich et al., 2014). Alternatively, it may suggest that late in the winter, when mean air
555 temperatures are beginning to increase, warming events are less likely to be followed by the
556 rapid drop in temperature which was highlighted by plot-level analysis as an important driver

557 of NDVI decline. Without this temperature drop, warming in later winter may simply
558 encourage earlier spring snowmelt and accelerate phenology, without damaging effects
559 (Meisingset et al., 2015). However, this appears to conflict with the association between large
560 NDVI reductions and warm exposure events during late winter, but the reason for these
561 apparently conflicting associations is not clear.

562

563 The regional-scale findings arise from analyses of change in TI-NDVI, yet regional-scale
564 climate metrics did not correlate with change in July NDVI (approximately peak biomass, or
565 peak NDVI). The peak season value of NDVI reflects the seasonal trajectory of photosynthetic
566 activity and can therefore help with interpretation of TI-NDVI (Park et al., 2016). However, it
567 is likely that the influence of altitudinal, latitudinal and coast-inland variability on the timing
568 of peak NDVI, combined with detection of this from just two MODIS images within a single
569 month, means that the genuine peak NDVI may not be well reflected in the methods used here.
570 TI-NDVI may make for better comparison of greenness among sites that have contrasting
571 phenology and timing of peak biomass. In addition, while winter extreme climatic events can
572 drive extensive vegetation mortality, and therefore biomass loss, they also frequently cause
573 severe stress and delayed phenology (Bjerke et al., 2017). Subsequent recovery from stress and
574 catch-up in phenology and/or growth (Koller, 2011; Treharne et al., 2018), would reduce
575 detection from peak season NDVI (Anderson et al., 2016), while the initial stress and
576 phenology impacts would be incorporated in (and likely detected in) TI-NDVI, which
577 correlates with total growing season productivity (Epstein et al., 2017).

578

579 **Plot-level compared with regional analyses**

580 Analyses at plot-level and regional scales, combined with correlation between plot-level and
581 remotely sensed NDVI (supporting information), indicated similar processes underlying the
582 greatest reductions in NDVI, in particular periods of unusual warmth and exposure during
583 winter, and especially during late winter. However, regional-scale analysis showed more
584 complexity compared to plot-level analysis; for example with colder temperatures during
585 exposure periods associated with greater TI-NDVI reductions in early winter. This illustrates
586 that, while the plot-level analysis focussed on the drivers of pre- and post-damage NDVI in
587 observed browning sites, when these drivers are scaled up to regional analysis, a wider range
588 of processes are involved in NDVI change. As TI-NDVI reflects cumulative productivity
589 across the May – August growing season, reductions in this indicator could reflect altered
590 phenology, and lower productivity in otherwise ‘undamaged’ vegetation, as well as the more
591 extreme ecological responses associated with extreme event-driven browning, such as
592 mortality and visible stress responses (Treharne et al., 2018). Assessing this greater range of
593 conditions driving TI-NDVI change is necessary to investigate the drivers of reductions in
594 greenness observed at landscape to pan-Arctic scales in recent years (Epstein et al., 2015, 2016;
595 Phoenix & Bjerke, 2016; Park et al., 2016). Nonetheless, having demonstrated that a small
596 number of climate metrics explain a high proportion of variation in NDVI across sites affected
597 by browning in the 2014 growing season, there is considerable potential for such simplified
598 approaches requiring a limited range of climate datasets to attribute drivers of browning and
599 be used in models to predict browning in the future.

600

601 **Conclusion**

602 This analysis has demonstrated that the severity of NDVI reductions, both across sites where
603 browning has been observed and at a regional scale, can be related to simple, process-based

604 climate metrics. These metrics reinforce ecological theory about the drivers underlying winter
605 climatic extreme event-driven browning, showing that prolonged periods of unusual warmth
606 and vegetation exposure during winter have negative consequences for NDVI. They also
607 provide novel and much-needed insight into how different climatological variables and timing
608 interact to produce greater or less severe browning. Looking forward, with further development
609 utilizing satellite data with medium to high spatial resolution like Sentinel-2 (10 meter), simple
610 climate metrics could be used to assess the impact of winter extreme climatic event driven-
611 browning on productivity at regional scales and improve predictions of changes in browning
612 frequency in the future.

613

614 **Highlights**

- 615 • New metrics quantified climatic drivers of extreme event-driven Arctic browning.
- 616 • These metrics explained up to 63% of variation in greenness at affected sites.
- 617 • Prolonged warmth or vegetation exposure in winter are associated with browning.
- 618 • Event metrics correlated with satellite greenness across Arctic Norway.

619

620 **References**

- 621 AMAP, 2017. Snow, Water, Ice and Permafrost in the Arctic (SWIPA) 2017. Arctic
622 Monitoring and Assessment Programme (AMAP), Oslo, Norway. xiv + 269.
- 623 Anderson, H. B., Nilsen, L., Tømmervik, H., Karlsen, S. R., Nagai, S. & Cooper, E. J., 2016.
624 Using ordinary digital cameras in place of near-infrared sensors to derive vegetation indices
625 for phenology studies of High Arctic vegetation. *Remote Sensing*, 8, 847,
626 doi:10.3390/rs8100847.
- 627 Altwegg, R., Visser, V., Bailey, L. D., & Erni, B., 2017. Learning from single extreme events.
628 *Phil. Trans. R. Soc. B*, 372, 20160141. <https://doi.org/10.1098/rstb.2016.0141>
- 629 Bailey, L. D., & van de Pol, M., 2016. Tackling extremes: challenges for ecological and
630 evolutionary research on extreme climatic events. *Journal of Animal Ecology*, 85, 85–96.
631 <https://doi.org/10.1111/1365-2656.12451>
- 632 Bjerke J. W., Karlsen S. R., Høgda K. A. et al., 2014. Record-low primary productivity and
633 high plant damage in the Nordic Arctic Region in 2012 caused by multiple weather events and
634 pest outbreaks. *Environmental Research Letters*, 9, 084006. <https://doi.org/10.1088/1748-9326/9/8/084006>.
- 636 Bjerke J. W., Treharne R., Vikhamar-Schuler D. et al., 2017. Understanding the drivers of
637 extensive plant damage in boreal and Arctic ecosystems: Insights from field surveys in the
638 aftermath of damage. *Science of The Total Environment*, 599–600, 1965–1976.
639 <https://doi.org/10.1016/j.scitotenv.2017.05.050>.
- 640 Bokhorst S., Bjerke J. W., Bowles F. W., Melillo J., Callaghan T. V., & Phoenix G. K., (2008).
641 Impacts of extreme winter warming in the sub-Arctic: growing season responses of dwarf shrub
642 heathland. *Global Change Biology*, 14, 2603–2612. <https://doi.org/10.1111/j.1365-2486.2008.01689.x>
- 644 Bokhorst, S., Bjerke, J. W., Street, L. E., Callaghan, T. V., & Phoenix, G. K., 2011. Impacts of
645 multiple extreme winter warming events on sub-Arctic heathland: phenology, reproduction, growth,
646 and CO₂ flux responses. *Global Change Biology*. 17, 2817–2830. <https://doi.org/10.1111/j.1365-2486.2011.02424.x>
- 648 Bokhorst, S. F., Bjerke, J. W., Tømmervik, H., Callaghan, T. V., & Phoenix, G. K., 2009.
649 Winter warming events damage sub-Arctic vegetation: consistent evidence from an

650 experimental manipulation and a natural event. *Journal of Ecology*, 97, 1408–1415.
651 <https://doi.org/10.1111/j.1365-2745.2009.01554.x>

652 Bourgeon, M. A., Gee, C., Debuissou, S., Villette, S., Jones, G., & Paloli, J. N., 2017. « On-
653 the-go » multispectral imaging system to characterize the development of vineyard foliage with
654 quantitative and qualitative vegetation indices. *Precision Agriculture*, 18, 293–308.

655 Burnham, K. P., & Anderson, D. R. (2002). *Model Selection and Multimodel Inference: A*
656 *Practical Information-Theoretic Approach*. Springer Science & Business Media, New York.

657 Denny, M. W., Hunt, L. J. H., Miller, L. P., & Harley, C. D. G., 2009. On the prediction of
658 extreme ecological events. *Ecological Monographs*, 79, 397–421. [https://doi.org/10.1890/08-](https://doi.org/10.1890/08-0579.1)
659 [0579.1](https://doi.org/10.1890/08-0579.1)

660 Easterling, D. R., Meehl, G. A., Parmesan, C., Changnon, S. A., Karl, T. R., & Mearns, L. O.,
661 2000. Climate extremes: observations, modelling, and impacts. *Science*, 289, 2068–2074.
662 <https://doi.org/10.1126/science.289.5487.2068>

663 Epstein H. E., Bhatt U.S., Raynolds M. K., et al. (2015) Tundra Greenness. In: Arctic Report
664 Card: Update for 2015 (eds Jeffries MO, Richter-Menge J., Overland J. E.). NOAA, Silver
665 Spring, MD. Available at: <http://www.arctic.noaa.gov/reportcard/>

666 Epstein H. E., Bhatt U.S., Raynolds M. K., et al. (2016) Tundra Greenness. In: Arctic Report
667 Card: Update for 2016 (eds Richter-Menge J., Overland J. E., Mathis, J. T.). NOAA, Silver
668 Spring, MD. Available at: <http://www.arctic.noaa.gov/reportcard/>

669 Graham, R. M., Cohen, L., Petty, A. A. et al., 2017. Increasing frequency and duration of Arctic
670 winter warming events. *Geophysical Research Letters*, 44, 6974–6983.
671 <https://doi.org/10.1002/2017GL073395>

672 Gutschick, V. P., & BassiriRad, H., 2003. Extreme events as shaping physiology, ecology, and
673 evolution of plants: toward a unified definition and evaluation of their consequences. *New*
674 *Phytologist*, 160, 21–42. <https://doi.org/10.1046/j.1469-8137.2003.00866.x>

675 Hadley, J. L., & Smith, W. K., 1989. Wind erosion of leaf surface wax in alpine timberline
676 conifers. *Arctic and Alpine Research*, 21, 392–398. <https://doi.org/10.2307/1551648>

677 Hadley, J. L., & Smith, W. K., 1986. Wind effects on needles of timberline conifers: seasonal
678 influence on mortality. *Ecology*, 67, 12–19. <https://doi.org/10.2307/1938498>

679 Hancock, M. H., 2008. An exceptional *Calluna vulgaris* winter die-back event, Abernethy
680 Forest, Scottish Highlands. *Plant Ecology & Diversity*, 1, 89–103.
681 <https://doi.org/10.1080/17550870802260772>

682 Hoover, D. L., & Rogers, B. M., 2016. Not all droughts are created equal: the impacts of
683 interannual drought pattern and magnitude on grassland carbon cycling. *Global Change*
684 *Biology*, 22, 1809–1820. <https://doi.org/10.1111/gcb.13161>

685 Hørbye J. 1882. Om frostskaeder paa barskoven [On frost damage to the conifer forests]. *Den*
686 *Norske Forstforenings Aarbog*, 99-105.

687 Horton, R. M., Mankin, J. S., Lesk, C., Coffel, E., & Raymond, C., 2016. A review of recent
688 advances in research on extreme heat events. *Current Climate Change Reports*, 2, 242–259.
689 <https://doi.org/10.1007/s40641-016-0042-x>

690 Jentsch, A., Kreyling, J., & Beierkuhnlein, C., 2007. A new generation of climate-change
691 experiments: events, not trends. *Frontiers in Ecology and the Environment*, 5, 365–374.
692 [https://doi.org/10.1890/1540-9295\(2007\)5\[365:ANGOCE\]2.0.CO;2](https://doi.org/10.1890/1540-9295(2007)5[365:ANGOCE]2.0.CO;2)

693 Jepsen, J. U., Biuw, M., Ims, R. A., Kapari, L., Schott, T., Vindstad, O. P. L., & Hagen, S. B.,
694 2013. Ecosystem impacts of a range expanding forest defoliator at the forest-tundra ecotone.
695 *Ecosystems*, 16, 561–575. <https://doi.org/10.1007/s10021-012-9629-9>

696 Knapp, A. K., Hoover, D. L., Wilcox, K. R. et al., 2015. Characterizing differences in
697 precipitation regimes of extreme wet and dry years: implications for climate change
698 experiments. *Global Change Biology*, 21, 2624–2633. <https://doi.org/10.1111/gcb.12888>

699 Koller, E. K., 2011. Controls on the growth of three subarctic dwarf shrubs along the
700 Kårsavagge catchment gradient. Chapter 2 in: *Impacts of environmental change on subarctic*
701 *dwarf shrub communities: landscape gradient and field manipulation approaches*. PhD thesis,
702 University of Sheffield.

703 Kudo, G., & Hirao, A. S., 2006. Habitat-specific responses in the flowering phenology and
704 seed set of alpine plants to climate variation: implications for global-change impacts.
705 *Population Ecology*, 48, 49–58. <https://doi.org/10.1007/s10144-005-0242-z>

706 Larcher, W., & Siegwolf, R., 1985. Development of acute frost drought in *Rhododendron*
707 *ferrugineum* at the alpine timberline. *Oecologia*, 67, 298–300.
708 <https://doi.org/10.1007/BF00384304>

- 709 Lloyd-Hughes, B., 2012. A spatio-temporal structure-based approach to drought
710 characterisation. *International Journal of Climatology*, 32, 406–418.
711 <https://doi.org/10.1002/joc.2280>
- 712 Mahecha, M. D., Gans, F., Sippel, S., et al., 2017. Detecting impacts of extreme events with
713 ecological in situ monitoring networks. *Biogeosciences*, 14, 4255–4277.
714 <https://doi.org/10.3929/ethz-b-000192472>
- 715 Meisingset, E. L., Austrheim, G., Solberg, E., Brekkum, Ø., & Lande, U. S., 2015. Effekter av
716 klimastress på hjortens vinterbeiter [Effects of climatic stress on red deer browsing –
717 development of bilberry after an extreme weather event during the winter of 2014]. Utvikling
718 av blåbærlyngen etter tørkevinteren 2014, NIBIO Rapport, 1 (64), 28 pp.
719 <http://hdl.handle.net/11250/2368503>
- 720 Niu, S., Luo, Y., Li, D., Cao, S., Xia, J., Li, J., & Smith, M. D., 2014. Plant growth and mortality
721 under climatic extremes: An overview. *Environmental and Experimental Botany*, 98, 13–19.
722 <https://doi.org/10.1016/j.envexpbot.2013.10.004>
- 723 Park, T., Ganguly, S., Tømmervik, H., Euskirchen, E.S., Høgda, K.A., Karlsen, S.R., Brovkin,
724 V., Nemani, R.R., & Myneni, R. B., 2016. Changes in growing season duration and
725 productivity of northern vegetation inferred from long-term remote sensing data.
726 *Environmental Research Letters*, 11, 084001. doi:10.1088/1748-9326/11/8/084001.
- 727 Parmentier, F.-J. W., Rasse, D. P., Lund, M., et al., 2018. Vulnerability and resilience of the
728 carbon exchange of a subarctic peatland to an extreme winter event. *Environmental Research*
729 *Letters*, 13, 065009. <https://doi.org/10.1088/1748-9326/aabff3>
- 730 Parmesan, C., 2006. Ecological and evolutionary responses to recent climate change. *Annual*
731 *Review of Ecology, Evolution, and Systematics*, 37, 637–669.
732 <https://doi.org/10.1146/annurev.ecolsys.37.091305.110100>
- 733 Pettorelli, N., Vik, J. O., Myrsterud, A., Gaillard, J.-M., Tucker, C. J., & Stenseth, N. C., 2005.
734 Using the satellite-derived NDVI to assess ecological responses to environmental change.
735 *Trends in Ecology & Evolution*, 20, 503–510. <https://doi.org/10.1016/j.tree.2005.05.011>
- 736 Phoenix, G. K., & Bjerke, J. W., 2016. Arctic browning: extreme events and trends reversing
737 arctic greening. *Global Change Biology*, 22, 2960–2962. <https://doi.org/10.1111/gcb.13261>

738 Phoenix, G. K., & Lee, J. A., 2004. Predicting impacts of Arctic climate change: past lessons
739 and future challenges. *Ecological Research*, 19, 65–74. <https://doi.org/10.1111/j.1440->
740 1703.2003.00609.x

741 Post, E., Forchhammer, M. C., Bret-Harte, M. S. et al., 2009. Ecological dynamics across the
742 Arctic associated with recent climate change. *Science*, 325, 1355–1358.
743 <https://doi.org/10.1126/science.1173113>

744 Printz, H. 1933. Granens og furuens fysiologi og geografiske utbredelse [The physiology and
745 geographical distribution of Norway spruce and Scots pine]. *Nyt Magazin for*
746 *Naturvidenskaberne B.* 73: 167-219.

747 Reichstein, M., Bahn, M., Ciais, P. et al., 2013. Climate extremes and the carbon cycle. *Nature*,
748 500, 287–295. <https://doi.org/10.1038/nature12350>

749 Rouse, J.W., Hass, R.H., Schell, J.A., & Deering, D.W., 1973. Monitoring vegetation systems
750 in the great plains with ERTS. In Proc. 3rd Earth Resources Technology Satellite (ERTS)
751 Symposium, Washington, DC, USA: NASA SP-351, NASA, Vol 1, 309–17.

752 Sakai, A., & Larcher, W., 2012. *Frost Survival of Plants: Responses and Adaptation to Freezing*
753 *Stress*. Springer Science & Business Media.

754 Sarojini, B. B., Stott, P. A., & Black, E., 2016. Detection and attribution of human influence
755 on regional precipitation. *Nature Climate Change*, 6, 669–675.
756 <https://doi.org/10.1038/nclimate2976>

757 Sillmann, J., & Roeckner, E., 2008. Indices for extreme events in projections of anthropogenic
758 climate change. *Climatic Change*, 86, 83–104. <https://doi.org/10.1007/s10584-007-9308-6>

759 Sippel, S., Zscheischler, J., & Reichstein, M., 2016. Ecosystem impacts of climate extremes
760 crucially depend on the timing. *Proceedings of the National Academy of Sciences*, 113, 5768–
761 5770. <https://doi.org/10.1073/pnas.1605667113>

762 Smith, M. D., 2011. An ecological perspective on extreme climatic events: a synthetic
763 definition and framework to guide future research: Defining extreme climate events. *Journal*
764 *of Ecology*, 99, 656–663. <https://doi.org/10.1111/j.1365-2745.2011.01798.x>

765 Solow, A. R., 2017. On detecting ecological impacts of extreme climate events and why it
766 matters. *Phil. Trans. R. Soc. B*, 372, 20160136. <https://doi.org/10.1098/rstb.2016.0136>

767 Stow, D. A., Hope, A., McGuire, D. et al., 2004. Remote sensing of vegetation and land-cover
768 change in Arctic tundra ecosystems. *Remote Sensing of Environment*, 89, 281-308.
769 <https://doi.org/10.1016/j.rse.2003.10.018>

770 Treharne, R., Bjerke, J. W., Tømmervik, H., Stendardi, L., & Phoenix, G. K. Arctic browning:
771 Impacts of extreme climatic events on heathland ecosystem CO₂ fluxes. *Global Change*
772 *Biology*, in press. <https://doi.org/10.1111/gcb.14500>

773 Ummenhofer, C. C., & Meehl, G. A., 2017. Extreme weather and climate events with
774 ecological relevance: a review. *Phil. Trans. R. Soc. B*, 372, 20160135.
775 <https://doi.org/10.1098/rstb.2016.0135>.

776 Van de Pol, M., Jenouvrier, S., Cornelissen, J. H. C., & Visser, M. E., 2017. Behavioural,
777 ecological and evolutionary responses to extreme climatic events: challenges and directions.
778 *Phil. Trans. R. Soc. B*, 372, 20160134. <https://doi.org/10.1098/rstb.2016.0134>

779 Vasseur, D. A., DeLong, J. P., Gilbert, B. et al., 2014. Increased temperature variation poses a
780 greater risk to species than climate warming. *Proceedings of the Royal Society of London B:*
781 *Biological Sciences*, 281, 20132612. <https://doi.org/10.1098/rspb.2013.2612>

782 Vikhamar-Schuler, D., Isaksen, K., Haugen, J. E., Tømmervik, H., Luks, B., Schuler, T. V., &
783 Bjerke, J. W., 2016. Changes in Winter Warming Events in the Nordic Arctic Region. *Journal*
784 *of Climate*, 29, 6223–6244. <https://doi.org/10.1175/JCLI-D-15-0763.1>

785 Williams, C. M., Henry, H. A. L., & Sinclair, B. J. (2015). Cold truths: how winter drives
786 responses of terrestrial organisms to climate change. *Biological Reviews*, 90, 214–235.
787 <https://doi.org/10.1111/brv.12105>

788 Wolf, S., Keenan, T. F., Fisher, J. B. et al., 2016. Warm spring reduced carbon cycle impact of
789 the 2012 US summer drought. *Proceedings of the National Academy of Sciences*, 113, 5880–
790 5885. <https://doi.org/10.1073/pnas.1519620113>

791 Zeppel, M. J. B., Wilks, J. V., & Lewis, J. D., 2014. Impacts of extreme precipitation and
792 seasonal changes in precipitation on plants. *Biogeosciences; Katlenburg-Lindau*, 11, 3083.
793 <https://doi.org/http://dx.doi.org/10.5194/bg-11-3083-2014>

794 Zscheischler, J., Mahecha, M. D., von Buttlar, J. et al., 2014. A few extreme events dominate
795 global interannual variability in gross primary production. *Environmental Research Letters*, 9,
796 035001. <https://doi.org/10.1088/1748-9326/9/3/035001>

797 Zscheischler, J., Mahecha, M. D., Harmeling, S., & Reichstein, M., 2013. Detection and
798 attribution of large spatiotemporal extreme events in Earth observation data. *Ecological*
799 *Informatics*, 15, 66–73. <https://doi.org/10.1016/j.ecoinf.2013.03.004>